



SPECTRAL ENERGY-EFFICIENT RESOURCE ALLOCATION IN MULTIPLE SYSTEMS

BHOODARAPU RAJENDER -Associate Professor & HOD,
Dept of ECE,

MOTHER THERESSA COLLEGE OF ENGINEERING & TECHNOLOGY, KARIMNAGAR, TS.

ABSTRACT: Wireless Sensor Networks (WSNs) have a broad application range in the area of monitoring and surveillance tasks. Among these tasks, disaster detection or prevention in environmental scenarios is one typical application for WSN. Disasters may for example be forest fires, volcano outbreaks or flood disasters. Here, the monitored events have the potential to destroy the sensor devices themselves. This has implications for the network lifetime, performance and robustness. While a fairly large body of work addressing routing in WSNs exists, little attention has been paid to the aspect of node failures caused by the sensed phenomena themselves. The EMA selects an energy-efficient channel access method that is either time-division multiple access (TDMA) or space-division multiple access (SDMA) for each sub band. For the SDMA, the near optimal number of SDMA time slots is derived. Numerical results verify that the EE of pure TDMA and SDMA can be significantly improved through the proposed EMA scheme.

Index Terms:- Energy efficiency (EE), channel access method, multiple access method, time-division multiple access (TDMA), space-division multiple access (SDMA), orthogonal frequency division multiple access (OFDMA).

I. INTRODUCTION

In wireless cellular networks, energy consumption is mainly drawn from BSs (base stations). According to the power consumption breakdown [1], BSs consume more than 50 percent of the power of a cellular network. In addition, the number of BSs is expected to be doubled by 2012 [2]. Thus, reducing the power consumption of BSs is crucial to green cellular networks. Efforts on greening cellular networks can be classified into three categories. The first category is to design power saving communication protocols that adjust the transmit power of the transceivers according to the traffic intensity. Radio access networks are dimensioned for peak hour traffic, and thus the utilization of the base stations can be very inefficient during the off-peak hours. The most intuitive idea is to switch off the transceivers when the traffic load is below a certain threshold for a certain time period [3]. When some base transceiver stations are switched off, radio coverage and service provisioning are taken care of by the devices that remain active. The BS switching problem can be formulated as an optimization problem that minimizes the number of active BSs while meeting the traffic load in the access network. Several algorithms and schemes have been proposed to solve the problem [4]–[6]. The second category is to design heterogeneous radio access networks which utilize a diverse set of base stations to improve spectral and energy efficiency per unit area. The network deployment featuring high density deployments of small, low power base stations achieve higher network energy efficiency than the sparse deployment of few high power base stations do. Etoh et al. [7] pointed out that heterogeneous network deployment will bring up to 50 percent reduction of the total BS power consumption. Samdanis et al. [8] examined the energy efficiency of cellular networks with joint macro and pico coverage, and showed that the joint deployment can reduce the total energy consumption by up to 60% in an urban area. The third category is to design off-grid BSs and

communication protocols to enable utilization of renewable energy in cellular access networks. Renewable energy such as sustainable biofuels, solar and wind energy are promising options to save the on-grid energy consumed by BSs and reduce the CO₂ footprint. Zhou et al. [9] proposed the HO (Hand Over) parameter tuning algorithm for target cell selection, and the power control algorithm for coverage optimization to guide mobile users to access to the BSs with natural energy supply, thus reducing the power expense and CO₂ emission.

On the other hand, high spectral efficiency (SE) is needed to support the growing demands of high data traffic. Orthogonal frequency division multiplex (OFDM) and orthogonal frequency division multiple access (OFDMA) are two popular spectral efficient systems. However, OFDM and OFDMA modulated signals exhibit high peak-to-average power ratio (PAPR), thus suffering from severe nonlinearity effects [4], [5] due to the nonlinearity of the PAs as illustrated in Fig. 2 (the details will be given in Section III). In practice, to circumvent the resulting performance degradation, input backoff (IBO) is implemented by reducing the power of the input at the PA, so that the amplification stays within the linearity region. While IBO allows high SE to be achieved, it can reduce the EE, because PAs are operate at high efficiency when it is near its power saturation point. Hence, a tradeoff exists between SE and EE when optimizing with respect to the PA. It is thus important to jointly characterize the role that a PA plays in both SE and EE of wireless communication systems. In this paper, the tradeoff of SE and EE for OFDM systems is analyzed by taking into account the impact of practical PAs. To provide tractable results, we assume that the nonlinearity of the PA is modeled by a soft limiter as shown in Fig. 2, i.e., the output is clipped to a constant if the input signal exceeds a threshold value, and experiences a linear scaling of its input otherwise [7]. We also propose a nonlinear transmit power model depending on PA types. As a consequence, we show that the practical SE-EE tradeoff



increases before a turning point and decreases rapidly after the turning point. In other words, the PA can support a narrow SE-EE tradeoff with only a limited range of SE.

II. EMA SYSTEM MODEL

We consider an M -antenna transmitter and U single antenna receivers (users) with N orthogonal frequency subbands. Denote a U -by- M channel matrix of subband $n \in N = \{1, \dots, N\}$ by H_n , whose (u,m) th element h_{um} is channel gain between the transmit antenna $m \in M = \{1, \dots, M\}$ and user $u \in U = \{1, \dots, U\}$. The channel is assumed to be static for T slots and vary in every T slots independently, i.e., a quasistatic channel with coherence time T . Each subband n supports K users where $K \leq T = \lfloor U/N \rfloor$. Throughout the paper, we assume that $KN \geq U$ and a scheduling function $\pi(n) = U_n$ assigns user $u \in U_n$ to subband n .

The EE of an EMA system is defined as

$$EE_2 = \frac{UR}{c \sum_{n \in N} P_{tx,n} + \max\{L_n\} P_{fix}}, \quad (1)$$

where R is a fixed target rate of each user, which implicitly involves an equality rate constraint, i.e., $R = (1 - \rho)Ru$, and is always feasible with allowing unlimited transmit power and ideal coding and decoding for each subband (user); c represents system inefficiency ($c > 1$) that is caused by overhead PC at RF circuits; $P_{tx,n}$ is transmit power on subband n ; P_{fix} is the fixed PC per time slot; L_n is the number of time slots used for transmission on subband n ; and $\max\{\cdot\}$ follows the fact that an RF chain should be turned on if there is at least one time slot to be transmitted over any subband. The EE-aware method maximizing EE_2 with an equality rate constraint is also optimal for EE maximization problem with an inequality rate constraint in a certain case. Furthermore, the equality rate constraint is reasonable in practice when we consider a capability-limited receiver that cannot recover a rate higher than the target due to the predesigned hardware limitation. We defer an MU EE maximization with inequality rate constraint to further work.

III. QoS-DRIVEN ENERGY-EFFICIENT POWER ALLOCATION

Assuming perfect CSI at the transmitter, an opportunistic power adaptation scheme can be developed to minimize the energy consumption per bit, or equivalently, maximize the transmitted data per unit energy, while satisfying a target delay-outage probability limit. The metric of interest in this case is the QoS-driven EE for delay-limited systems defined as the ratio of the EC to the total expenditure power. The total power dissipation model includes a constant circuit power PC and a transmission power scaled by the power amplifier efficiency ϵ . The rate-independent circuit power PC corresponds to the power dissipated in device electronics. Accordingly, the QoS-driven EE is mathematically represented as

$$EE(\theta) = \frac{-\frac{1}{\alpha} \log_2 \left(\mathbb{E}_\gamma \left[\prod_{n=1}^N \left(1 + \frac{NP_n(\theta, \gamma)}{K_L} \right)^{-\frac{1}{\alpha}} \right] \right)}{P_C + \epsilon \cdot \mathbb{E}_\gamma \left[\sum_{n=1}^N P_n(\theta, \gamma) \right]}$$

where $K_L \equiv \text{PLN}0B$ is a loss factor denoting the product of path loss and noise power. In order to normalize the system

performance with respect to KL, we define $P_n(\theta, \gamma) \equiv P_n(\theta, \gamma) / K_L$ as the ratio of the transmit power at the n th subcarrier to the path loss and noise power. Thus, the EC formula can be expressed as

$$E_c(\theta, P^R(\theta, \gamma)) = -\frac{1}{\alpha} \log_2 \left(\mathbb{E}_\gamma \left[\prod_{n=1}^N \left(1 + N \cdot P_n^R(\theta, \gamma) \gamma_n \right)^{-\frac{1}{\alpha}} \right] \right),$$

where $P^R(\theta, \gamma) = [P_1^R(\theta, \gamma) \ P_2^R(\theta, \gamma) \ \dots \ P_N^R(\theta, \gamma)]$, where $P^R(\theta, \gamma)$ is the total power spend over a bandwidth B , γ is the channel power gain of a single carrier flat-fading and $PCR = PC / \epsilon K_L$ is the normalized circuit power. The corresponding subcarrier power allocations can be obtained using [4], [14] as

$$P_n^R(\theta, \gamma_n) = \frac{1}{N} \left[\frac{1}{\delta^{\frac{1}{\alpha+K}} \gamma_n^{\frac{1}{\alpha+K}}} - \frac{1}{\gamma_n} \right]^+, \quad n \in N_0,$$

where $[x]^+ = \max(0, x)$ and δ is a cutoff threshold that can be found numerically to maximize (10). It was shown in [3] that maximizing the EC at each subchannel independently, using the optimal power adaptation policy for the single channel transmission, does not yield a SE-optimal power scheme. In fact, by using the independent allocation over N i.i.d. subchannels, the resulting EC, $E(N) c(\theta)$, converges to zero as $\theta \rightarrow \infty$ for any finite N . In turn, by applying the independent EE optimization approach in (11) to our underlying multicarrier system, the achievable EE at very stringent θ is expected to converge to zero for any finite power. Hence, independently optimizing the power allocated to the subcarriers can not yield an EE-optimal power scheme. In the following sections, we propose an optimal EE power allocation policy where the power is jointly distributed over both frequency and time. B. Jointly Optimal Energy-Efficient Power Allocation Policy without Transmit Power Constraint First, the unconstrained optimization problem is tackled without considering any input transmit power constraint, serving as a milestone towards finding an EE-optimal power allocation subject to an average sum power constraint. To maximize the QoS-driven EE, the optimization problem can now be formulated as follows

$$EE^{opt}(\theta) = \max_{P_n^R \geq 0, n \in N_0} \frac{1}{\epsilon K_L} \cdot \frac{E_c(\theta, P^R(\theta, \gamma))}{P_C + \mathbb{E}_\gamma \left[\sum_{n=1}^N P_n^R(\theta, \gamma) \right]}$$

In [15], a mathematical framework called fractional programming is provided to solve optimization problems where the objective function is a ratio of two real-valued functions. Specifically, the authors showed that a broad class of EE maximization problems can be solved efficiently provided the rate is a concave function of the transmit power.

IV. EMA IN A SINGLE-SINK SCENARIO

The simulations for the evaluation of the proposed routing method were performed using the network simulator OPNET [11] with the simulation layout described in the previous section of this paper. The MAC (Medium Access Control) and PHY (Physical) layers in the node model are based on the Open-ZB [10] implementation (version 1.0) of the 802.15.4 stack. Different from the original Open-ZB model, the MAC layer was modified to support an adhoc



mode with unslotted CSMA/CA instead of the original PAN-coordinated mode. This modified MAC layer was first used in work reported in [13]. We simulated the scenario for a model time of 90 minutes. Several statistics were collected and are shown in the following. OLSR (Optimized Link State Routing) was chosen as a protocol for comparison. The existing OLSR implementation of OPNET's wireless module was used and the PHY and MAC layers were replaced with the 802.15.4 layers. OLSR is a standard proactive routing protocol for ad-hoc networks and can therefore be considered as the base line protocol for proactive routing studies. To achieve comparability, the route lifetime is set to 30 seconds in both, EMA and OLSR simulation scenarios. EMA beacons are transmitted at intervals of 15 seconds, OLSR hello messages at the same intervals. OLSR topology control (TC) messages are transmitted at 30 second intervals. The applied temperature model is simple: As long as a node is not exposed to fire, its temperature values are normally distributed with a mean of 20 degrees Celsius and a standard deviation of one degree Celsius. When the node becomes exposed to the fire, a linearly growing offset is added to the node's temperature value. Figure 2 shows the temperature curve at sensor node 1, a node that is located close to the fire breakout location. It can be seen that in the applied temperature model, the temperature increases quickly when the fire reaches the node, which in the illustrated case happens at ca. 1900 seconds of model time. Within a short time, the maximum temperature threshold is reached and the node dies.

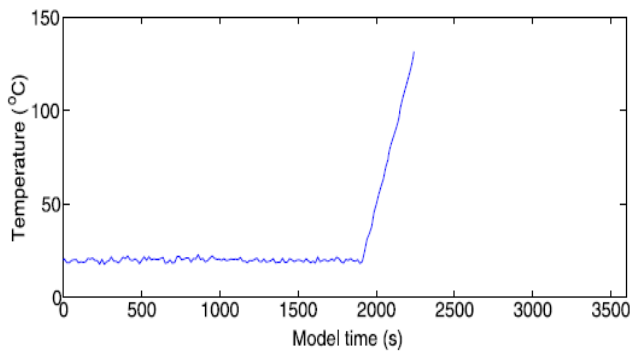


Fig. 2 Temperature graph according to the applied temperature model, at the example of sensor node 1

This temperature graph is shown to illustrate the conditions the nodes experience when the fire reaches them. Real temperature curves might have a smoother nature, which would make it even easier for a health-aware routing protocol to adapt to the changing conditions.

Figure 3 shows the packet reception statistics from the individual sources (sensor nodes) at the sink. The values on the ordinate are the IDs of the sensor nodes. Each cross marks the reception of an individual packet from the respective source at the sink. A continuous incoming flow of data from each node is visible (although the interarrival times vary in some cases). The flow of data stops abruptly when the node dies. The EMA algorithm performs as intended as data from all sensor nodes reaches the sink, and inflow of data packets continues until sensor nodes die. As Fig. 3 does not directly show how much of the generated

traffic is received at the sink, the incoming packet rate is compared to the generation rate in Fig. 4.

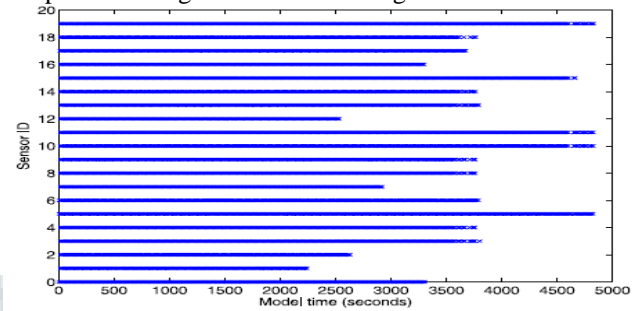


Fig. 3 Incoming packet flows at the sink

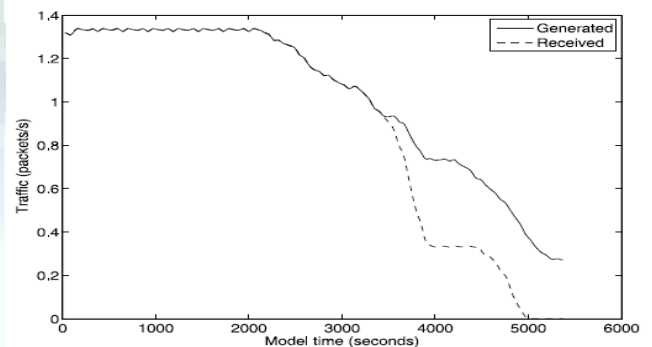


Fig. 4 Traffic generated and received at the sink in packets/s (EMA routing)

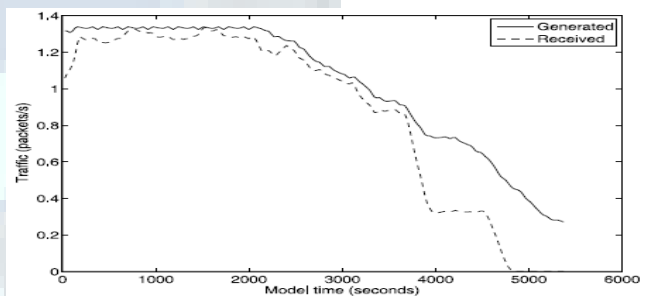


Fig. 5 Traffic generated and received at the sink in packets/s (OLSR routing)

The death of nodes leads to less data traffic being generated and being received at the sink. This can be seen in the packet generation and reception rates shown in Fig. 4. The solid curve shows the generation rate, the dashed curve shows the reception rate. Both curves show moving average values in a 250 s time window, so that the curves are smoother and the difference between generation and reception is more visible. For comparison, the packet generation and reception rates were also measured in the OLSR simulation and are shown in Fig. 5. From Fig. 4, it can be seen that until around 3500 seconds of model time, the incoming packet rate is on the level of the generated rate, which is 1.33 packets/s when all nodes are alive (see Sect. 4). The steep drop that follows is caused by the failure of sensor node 17. When this node fails, the nodes in the upper right area cannot reach the sink any more. The second significant drop is the failure of sensor node 5, after which no node can reach the sink any more (sensor node 0, which is also close to the sink, has already failed before). Figure 3 shows quite clearly that there are several nodes from which no more data is received when node 17 fails, and similarly for the failure of sensor node 5. These results show that the



protocol succeeds in changing the routing in time before transmission problems occur, so that the nodes are able to deliver their data as long as there is a way to reach the sink. The OLSR results shown in Fig. 5 show a lower and varying incoming packet rate throughout the simulation. This means there are less successful transmissions in the OLSR scenario. Similar observations were made for AODV (see [14]). The reason for these problems even in the case of a static network is that neither AODV nor OLSR use context values such as the RSSI values. This leads to potential elections of routes with low RSSI, which in turn causes transmission failures. Another performance measure that was recorded in the simulations were the end-to-end delays. These were not

broadcasted, but not forwarded, TC messages are flooded into the network, causing a significant signaling overhead. The comparisons show clearly that the proposed EMA routing approach is superior to the OLSR routing protocol in the given scenario.

V. EMA WITH MULTIPLE SINKS

To ensure a higher probability of successful data delivery, it can be advantageous to add multiple redundant sinks to the network. Redundant here means that all sinks have exactly the same functionality, so that any of them can act as receiver for the sensor data.

In OLSR, this is problematic as the sensor nodes need to specify a destination address when they transmit their data. This means the sinks either have to have the same address, or the nodes have to multicast their data. Having multiple nodes with the same address causes further protocol problems, as OLSR is not designed to handle this. Multicasting, on the other hand, increases the overall traffic significantly as in this case sensor nodes need to perform multiple transmissions.

In contrast to the problems that occur with multiple sinks in an OLSR network, EMA does not have these problems, as the sensor nodes just elect their best neighbor and do not have to care about to which sink the transmission is directed. If there are multiple sinks, all of the sinks send out their beacons. The sensor nodes may then receive beacons from multiple sinks and just elect the best one as their best neighbor. To verify this, the scenario depicted in Fig. 1 is modified by adding a second sink in the upper right corner and a third sink in the lower left corner. Adding the sinks to the corners is a reasonable placement in the given scenario, as the corners of the forest area are probably the physically most accessible locations. Figure 8 shows the generated and delivered traffic in case of 1, 2 and 3 sinks. It can be seen that by placing the second sink in the upper right corner, the failure of sensor node 17 does not have the impact any more that it had in the single sink case. Similarly, the impact of the sensor node 5 failure gets eliminated by the third sink in the lower left corner. When there are sinks in 3 corners of the simulation area, all sensor nodes can deliver their data throughout the complete simulation. The energy consumption throughout the network is shown in Fig. 9. Interestingly, the consumption in the cases of 1 and 2 sinks is virtually identical. The reason is that shorter routes in the second sink's vicinity compensate for the additional energy that is spent for the second sink's beacons and their forwarding.

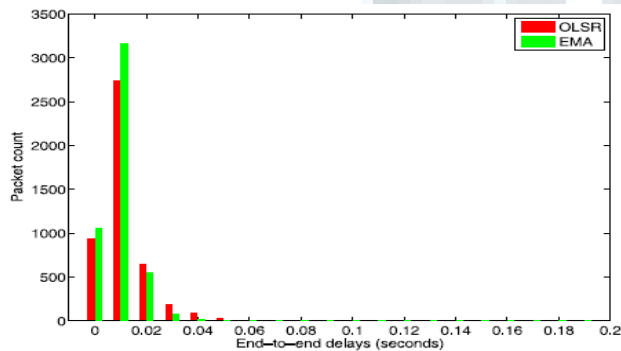


Fig. 6 End-to-end delay histogram for EMA and OLSR

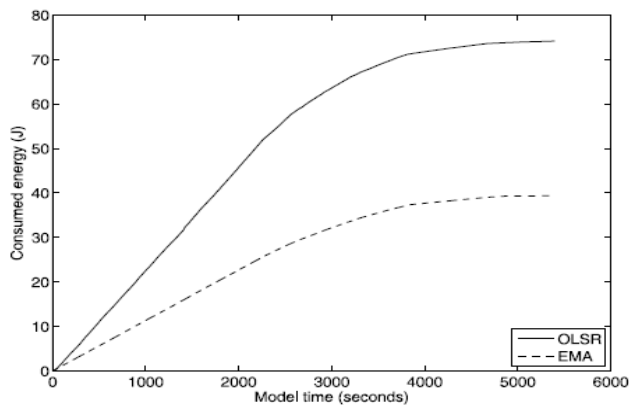


Fig. 7 Network-wide energy consumption

recorded for each source node separately, but across all source nodes. Figure 6 shows a histogram of the end-to-end delays for both routing methods. The histogram depicted in Fig. 6 shows that generally, the delays are quite similar for both algorithms, with a minor advantage on the side of the proposed EMA algorithm. However, in comparison to the measurement intervals of 15 seconds, the delays are negligible for both algorithms. The third recorded performance measure is energy consumption.

The comparison of the consumption for EMA and OLSR is shown in Fig. 7. The graphs here show the overall energy consumed in the network since the start of the simulation.

A significant difference can be seen in these energy consumption graphs. EMA consumes much less energy, approximately half of what is consumed by OLSR. This is caused by the differences in how the route tables are proactively maintained: While EMA uses beacon forwarding and only forwards beacons that are relevant, OLSR uses two types of regularly transmitted messages: hello messages and TC messages. While hello messages are

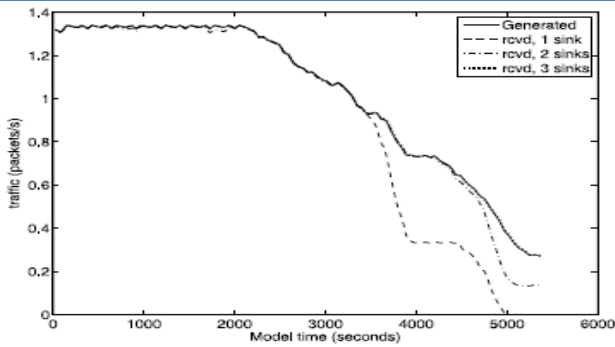


Fig. 8 Traffic generated and received at the sink (EMA routing with multiple sinks)

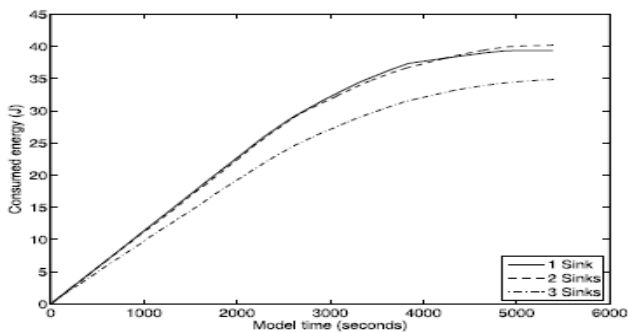


Fig. 9 Network-wide energy consumption with multiple sinks

In the case of 3 sinks, the overall consumed energy is less than in the other two cases, although the addition of each sink means one additional beacon transmitter. Here, the nodes that are located near the third sink have now also shorter routes towards a sink. This overcompensates for the additional beacon overhead.

VI.CONCLUSION

This paper attempts to present major studies of disk energy optimization techniques, such as adopting architectural mechanisms such as spinning down idle disks, Traditional Power Management (TPM) etc which is available in the literature. These conventional energy optimization techniques form the basis for the new innovation of the effective power consumption approaches. Most of the stabilization techniques available in the literature operate in reactive manner, and moreover there is significant performance penalties. We have proposed a routing approach that proactively adapts routes in a wireless sensor network based on information on node-threatening environment influences. The approach, called Environmental Monitoring Aware (EMA) routing, has been evaluated by computer simulation and has demonstrated good performance in the considered forest fire scenario. With respect to the considered network and performance parameters, it outperforms the proactive OLSR routing algorithm. In particular, EMA routing can support multiple sinks with no additional overhead. The routing approach is also more flexible than standard protocols in that additional environmental parameters can be added simply to the routing algorithm to adapt the approach to a wide range of applications. Further research will include evaluation in further scenarios. A reactive variant of EMA

will be investigated as well, and EMA will also be investigated in scenarios with sensor node mobility.

REFERENCES

1. Heinzelman, W. B., Chandrakasan, A. P., & Balakrishnan, H. (2002). An application-specific protocol architecture for wireless microsensor networks. *IEEE Transactions on Wireless Communications*, 1(4), 660–670.
2. Intanagonwivat, D., Govindan, R., Estrin, D., Heidemann, J., & Silva, F. (2003). Directed diffusion for wireless sensor networking. *IEEE/ACM Transactions on Networking*, 11(1), 2–16.
3. Kalpakis, K., Dasgupta, K., & Namjoshi, P. (2002). Maximum lifetime data gathering and aggregation in wireless sensor networks. In *Proceedings of the 2002 IEEE international conference on networking*.
4. Kulik, J., Heinzelman, W., & Balakrishnan, H. (2002). Negotiation based protocols for disseminating information in wireless sensor networks. *ACM Wireless Networks*, 8, 169–185.
5. Liang, Q., & Ren, Q. (2005). Energy and mobility aware geographical multipath routing for wireless sensor networks. In *Proceedings of the IEEE wireless communications and networking conference 2005* (pp. 1867–1871).
6. Lindsey, S., & Raghavendra, C. S. (2002). PEGASIS: power efficient gathering in sensor information systems. In *Proceedings IEEE aerospace conference* (Vol. 3, pp. 1125–1130).
7. Manjeshwar, A., & Agrawal, D. P. (2001). TEEN: a routing protocol for enhanced efficiency in wireless sensor networks. In *Proceedings of the 15th international parallel and distributed processing symposium* (pp. 2009–2015).
8. Mascolo, C., & Musolesi, M. (2006). SCAR: context-aware adaptive routing in delay tolerant mobile sensor networks. In *Proceedings of the 2006 international conference on wireless communications and mobile computing* (pp. 533–538).
9. Minseok Song; Wanhyung Ryu; Jeong Seop Sim; “Reducing disk power consumption in portable media players”, 2010 8th IEEE Workshop on Embedded Systems for Real-Time Multimedia (ESTIMedia), Page(s): 81 – 89, 2010.
10. Qingbo Zhu; David, F.M.; Devaraj, C.F.; Zhenmin Li; Yuanyuan Zhou; Pei Cao; “Reducing Energy Consumption of Disk Storage Using Power-Aware Cache Management”, Page(s): 118, 2004.

AUTHOR’S PROFILE:



BHOODARAPU RAJENDER, He is having well experience in teaching in Graduate and PG level and present he is working as Associate professor and Head of the Department for ECE Mother Theresa College Of Engineering & Technology, Karimnagar, Ts, India.